What earthquake would be amplified more at a soil site? - A study of seismic amplification in Parkway, New Zealand

NZSEE 2001
Conference

Jiashun Yu
Institute of Geological and Nuclear Sciences, Lower Hutt

J. J. Taber
School of Earth Sciences, Victoria University of Wellington

ABSTRACT: To understand what earthquake would be amplified more in a Quaternary sedimentary basin, ten earthquakes recorded at the Parkway basin, Wainuiomata, New Zealand, were studied. The ground motion amplification in the basin of an earthquake was quantified using spectral ratios of recordings from soil sites to rock sites. The spatial coherence of seismic waves was also calculated for each event. The results demonstrate that there is a correlation between the amplification and the coherence of the seismic waves at the fundamental resonant frequency -- the more coherent the waves, the greater the ground motion amplification in the basin. This observation was supported by three-dimensional modelling of the ground motion in the basin. The modelling showed that coherent SH or SV incident waves were amplified significantly more than randomly incident waves. This suggests that ground motion in a basin will be amplified more for an earthquake when the waves of the earthquake are more coherent.

1 INTRODUCTION

The amplification of ground motion within sedimentary basins has been a major factor in the damage distribution in many earthquakes. Observations show that the amplification for a site varies from event to event (Field & Jacob 1995, Haines & Yu 1997). It has been proposed that the degree of amplification is affected by the spatial coherence of the incident waves, as well as being controlled by the local geology of the observation site (Yu 1996a, Haines & Yu 1997). Thus it may be the variable degree of coherence of incident seismic waves for different earthquakes that causes the variability of amplification of seismic ground motion.

In this paper, the variability of amplifications and the spatial coherence of seismic waves is characterised for 10 earthquakes recorded in the Parkway basin. This enables the determination of the correlation between the amplification and coherence. Then three-dimensional modelling of seismic waves in the basin with different coherences is discussed. The modelling provides a test as to whether the degree of seismic amplification in the basin is correlated with the coherence of the waves.

2 OBSERVATIONS

2.1 *Data*

Parkway, Wainuiomata, is a suburban residential area of Wellington, New Zealand (Figure 1) in a flat-floored 400 m wide alluvial basin (Figure 1). A dense temporary seismic array was deployed in Parkway in 1995 to study the seismic amplification (Yu 1996b, Beetham 1999, Chavez-Garcia et al. 1999). There were 20 soil sites in the basin and 4 rock sites surrounding the basin that recorded up to 85 events over a 2-month period.

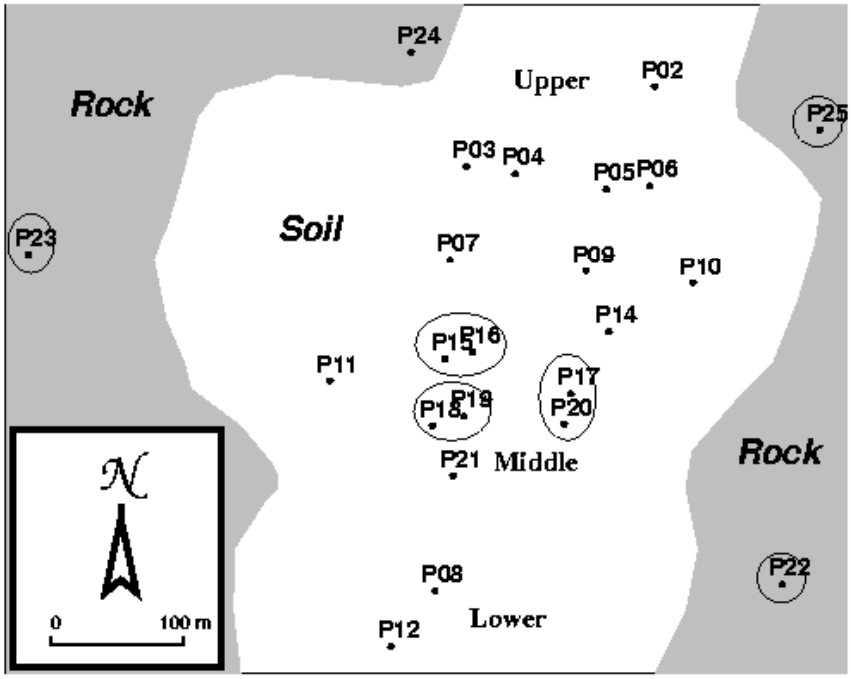

Figure 1. The Parkway Basin and the seismic sites occupied in the 1995 deployment. The circled sites were the ones used for this study. Sites P22, P23 and P25 were on rock (gray shaded area) surrounding the basin. These were used as the reference sites. The other 6 sites were on the flexible soil in the basin. Upper, Middle, and Lower refer to the computer modelling discussed in Section 3.

In order to use a uniform set of recordings for the study, 10 earthquakes that were recorded at six soil sites in the basin and 3 rock sites surrounding the basin were selected from the 1995 data set. The magnitudes of these earthquakes ranged from 2.5 to 5.2 and the hypocentral distances range from 17 to 436 km. The horizontal PGA of the earthquakes observed in the basin ranged from 0.013 to 0.108 m/s^2 (Table 1).

Table 1. Parameters of the 10 earthquakes

Num	Year	Mon	Day	Hr	Min	Sec	Lat	Long	Depth	Dist	Mag	HPGA
1	1995	08	04	18	15	56.4	41.61	175.37	24	59	3.3	.0023
2	1995	08	05	13	21	52.0	41.32	174.42	40	59	2.9	.0019
3	1995	08	06	12	52	28.2	41.08	174.48	40	58	3.1	.0038
4	1995	08	98	10	04	54.7	40.31	173.52	195	251	4.1	.0041
5	1995	09	03	15	57	37.2	41.10	174.85	56	58	3.2	.0105
6	1995	09	03	17	51	39.2	37.87	176.67	160	434	5.2	.0085
7	1995	09	11	08	53	35.3	40.47	176.47	42	160	4.6	.0085
8	1995	09	12	12	55	39.8	41.14	175.08	5	17	2.5	.0057
9	1995	09	13	14	31	33.2	40.96	174.99	29	43	3.1	.0108
10	1995	09	14	13	45	26.7	42.03	173.91	21	123	3.5	.0013

* Dist = hypocentral distance (km); HPGA = horizontal PGA (m/s^2)

2.2 *Analysis*

The simplest way to quantify the earthquake-to-earthquake variation in amplification at a soil site is to evaluate the range in spectral ratios of that site relative to the reference rock sites due to different earthquakes. To get a more statistically stable result, recordings from all the soil sites can be combined to characterise the variation. Each ratio is normalised by the mean of the peak amplitudes of the spectral ratios for all the events at that site before calculating the average over the sites. This factor is referred to here as the strength of amplification.

The spatial coherence of seismic wavefields is defined as the coherence of the same components of recordings at two separate sites:

$$Coh_{ij}(f) = \frac{\left|F_i(f) + F_i(f)\right|^2}{\left|F_i(f)\right|^2 + \left|F_j(f)\right|^2} - 1 \qquad (1)$$

where F_i is the amplitude spectrum of the shear wave part of the north or east component recorded at the ith site and F_j is the amplitude spectrum of the same component at the jth site. The 6 soil sites fall into three pairs, with a site separation of about 25 m for each pair. The function is a measure of the similarity of the wave at the two sites of the pairs.

As the study is focussed on the amplification of the shear waves, the spectral ratios, strength functions of amplification and the coherence functions were all calculated using the shear wave parts of the recordings. The time duration of the series used for calculating the spectral ratios and strength of amplification was 50 seconds starting just before the shear wave arrival. For calculating the coherence functions only the first 6 seconds were used. This is normally the most coherent part of a recording as the later arrivals have too much scattering involved and are less useful for the analysis.

The amplification of seismic ground motion in the basin is shown by the spectral ratios from the six soil sites relative to the average of the three reference rock sites (Figure 2). The amplification is similar at the six sites. The fundamental resonant frequency is 1.7±0.1 Hz and the peak amplification is 8.5±1.5. There is significant variation in amplification at each site due to different events. Note that the event variation range is consistent across all the six sites.

The strength of amplification in the basin was calculated for each of the 10 events. As well, the spatial coherence was first calculated for each component of each basin site pair (P15-P16, P17-P20 and P18-P19) for each event. Then the average for each event was calculated using the six functions for the event (three sites with two components each). The peak strength was determined from the strength function for each event and the coherence value was noted for each event at the frequency where the peak strength occurred. Comparing the standard deviations with the ranges of coherence and strength (Figure 3) shows that the errors are relatively large. However there is a clear correlation shown by the mean values between strength and coherence, with strength increasing with coherence.

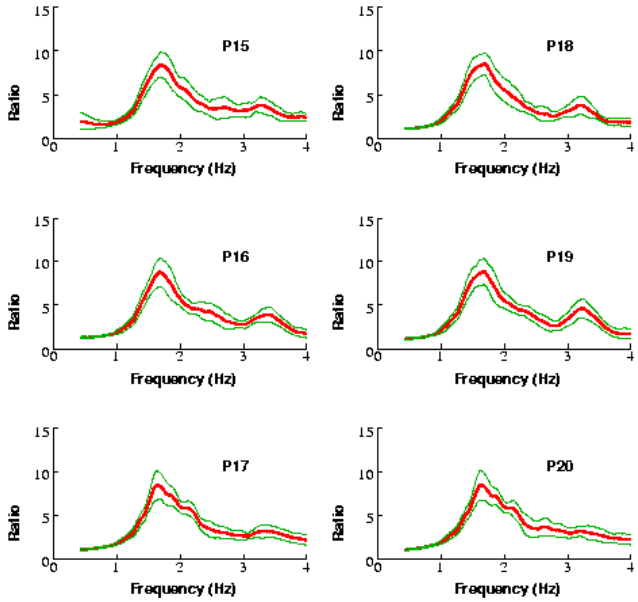

Figure 2. The spectral ratios of the six basin sites relative to the average of the three reference rock sites. The dark line is the mean ratio of all events and the two thin lines are ± one standard deviation. Each spectrum was smoothed using a 0.2 Hz half-width triangular moving window.

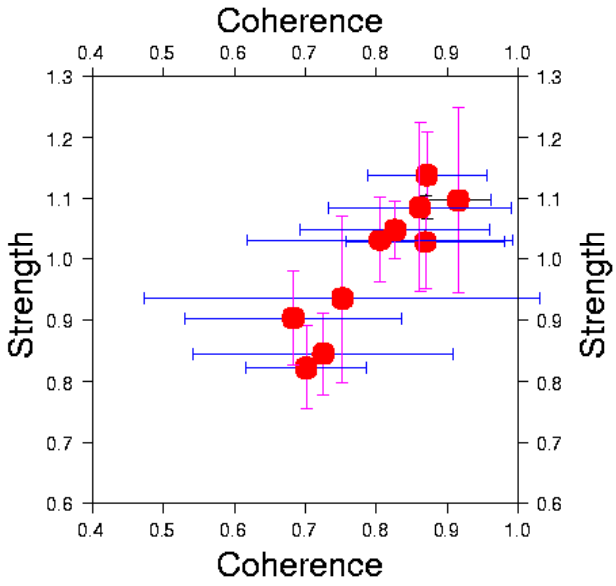

Figure 3. Correlation between spatial coherence and the strength of amplification of the seismic waves. Filled circles show the strength and mean coherence for each event. Bars show ± one standard deviation of both parameters.

3 THREE-DIMENSIONAL MODELLING

3.1 *Model*

Geotechnical investigations have been carried out in the Parkway basin and the adjacent Wainuiomata area (Begg et al. 1993, Barker 1996, Duggan 1997, Sutherland & Logan 1998). However they lack the resolution to constrain a detailed three-dimensional model for the basin, so a simple two layer model was developed using the existing information as a starting point. The undetermined physical parameters for the layers were estimated by one-dimensional SH wave modelling (Yu 1996a) with observed resonant frequencies and amplitudes as constraints. The modelling was performed at three indicative sites in the basin (labelled Upper, Middle and Lower in Figure 1).

Using the one dimensional models determined at these three sites, a three dimensional model for the basin was built by extrapolating the parameters of the one dimensional models across the basin. The three dimensional model is 700 by 700 metres laterally, and 68 metres in thickness (Figure 4 and Table 2).

Table 2. Physical parameters for the Parkway basin.

Layers	Depth (m)	Density (g/cm^3)	Vs (m/s)	Vp (m/s)	Qs	Qp
Top layer	0	1.7-1.9	100-220	1500	15	50
Bottom layer	1-16	2.0	500	2000	50	100
Basement	38-65	2.6	1500	3200	inf	inf

3.2 *Modelling*

The purpose of the modelling was to test if there is a correlation between the amplification and coherence of the waves in the basin. Therefore two kinds of wavefields were separately synthesised, one representing a coherent case and the other a random case. Vertically incident pure SH and SV waves were separately used as the coherent case, and the superposition of random SH and SV incident waves from all spatial directions as a random case.

The modelling of the random wavefields in a basin was a two step process. First a set of 69 deterministic fundamental wavefields in the basin was calculated for each frequency using the Riccati-Haines approach (Yu 1996a). Then these wavefields were randomly combined according to the possible incidence distribution (Yu 1996a). The distribution of incidence angles is heavily weighted towards near vertical incidence. This was to mimic the observation that most waves propagate into the basin in a near-normal direction as the wave velocity in the basement is significantly lower than the deeper crust where the waves originate. The total of the random weights over the whole space for a random event has a mean of 1. This provides a base for comparison with the deterministic pure incident wavefields. The modelling was performed for 6 frequencies ranging from 1.5 to 2.0 Hz, with an increment of 0.1 Hz.

Shown in Figure 5 is the comparison of the amplification patterns of the wavefields in the basin due to different incident waves. The response wavefields in the basin due to each pure type of incident wave are seen to be dominated by the incident wave polarisation. Converted waves are also seen in the basin in the other components, but their amplitudes are relatively small. For the waves due to random incident waves, the energy is evenly distributed in the two horizontal components. Comparing the random waves with those due to pure types of incident waves, the amplitude of the waves in the basin due to random wavefields is significantly smaller. In other words, the randomness in the incident waves tends to reduce their amplification in the basin.

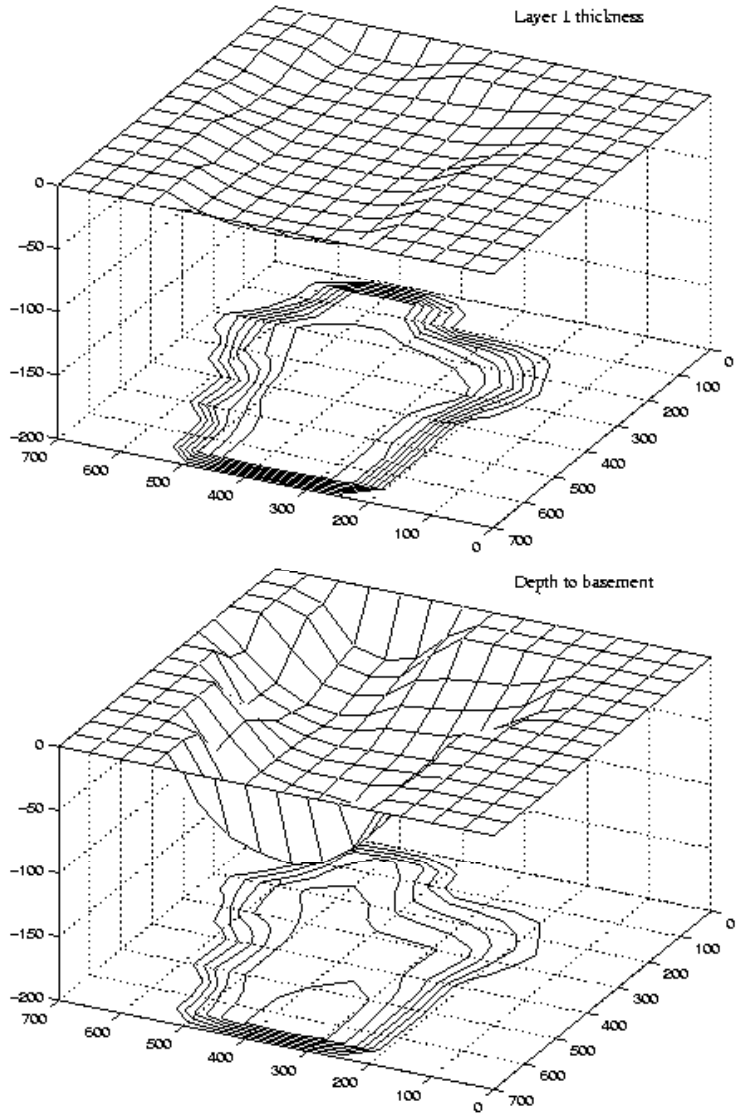

Figure 4. Model geometry. A contour plot is shown at the bottom of each box. Top: bottom interface of Layer 1, contour interval 2 m. Bottom: depth to basement, contour interval 10 m.

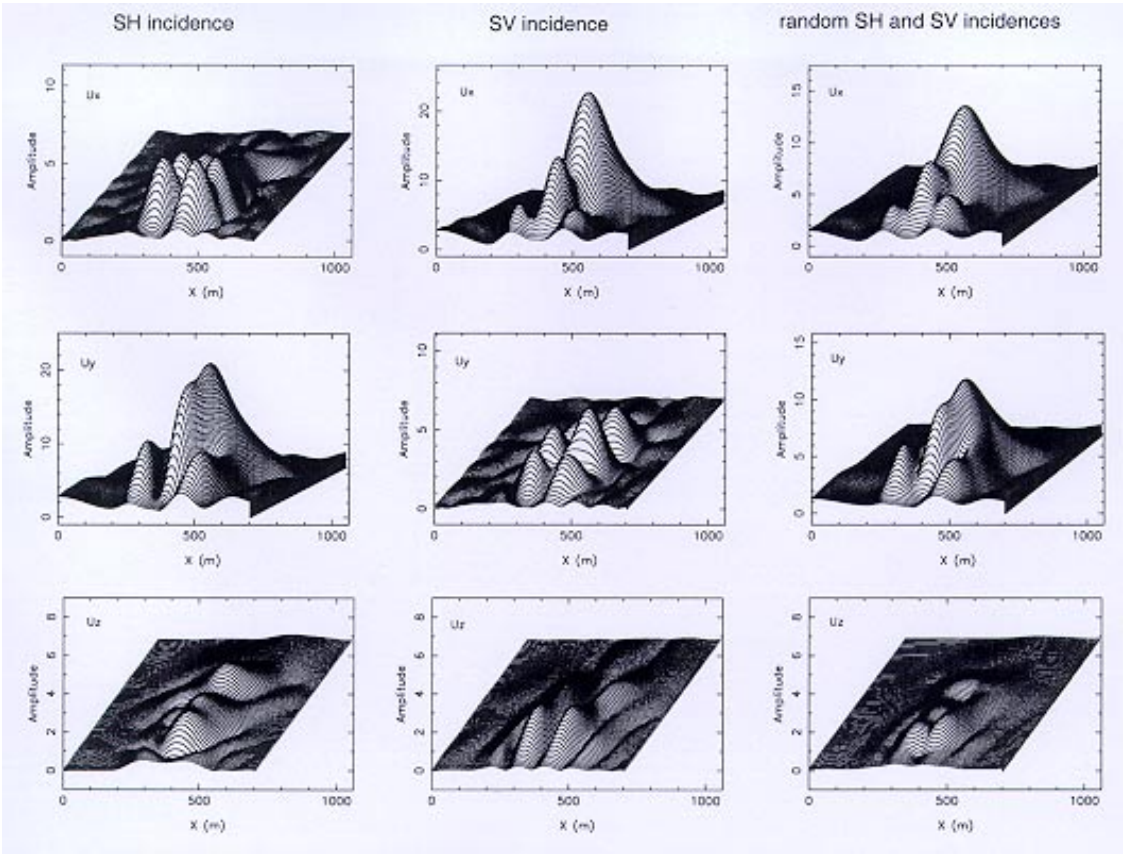

Figure 5. The amplitude of the synthetic wavefields at the ground surface of the basin due to different incident waves at 1.7 Hz. The first column is that due to normal incident SH waves. The second column is that due to normal incident SV waves. The third column is that due to random incident waves of SH and SV types from all spatial directions with various incident angles. There are three blocks in each column. From the top to the bottom, each block shows the x (east), y (south) and z (upward) components. The normal incident SH and SV waves are defined to be polarised in the y and x components, respectively. Note the varying amplitude scales in the plots.

In order to compare the model results with the recorded data, the amplification and coherence of the synthetic waves were calculated in the similar way as for the observation. For the synthetic data, an average was taken over a grid in the central basin where the six observed sites were located, with a spacing similar to that of the pairs of soil sites used for calculating the coherence functions for the observed data. The average amplification and coherence functions for each synthetic wavefield are listed in Table 3 for the calculated frequencies nearest the resonant frequency. The table shows that the wavefields due to pure SH or SV incidence are highly coherent in the dominant components, and these components are also largely amplified in the basin compared with the random wavefield. This contrast between the two kinds of wavefields is largest at the resonant frequency of 1.7 Hz. The contrast at this frequency is shown in Figure 6. This modelling result is consistent with the observed correlation between coherence and strength of amplification.

Table 3 Amplification strength and coherence of waves in the Parkway basin.

		Pure SH		Pure SV		Random SH+SV	
Hz		x	y	x	y	x	y
1.6	Coh	0.357	0.992	0.999	0.354	0.956	0.924
	Amp	0.484	10.652	11.520	0.369	6.150	5.348
1.7	Coh	0.402	0.985	0.995	0.231	0.937	0.899
	Amp	0.886	13.113	15.093	0.697	8.026	6.633
1.8	Coh	0.505	0.963	0.978	0.607	0.901	0.862
	amp	1.512	12.249	12.937	1.196	6.941	6.264

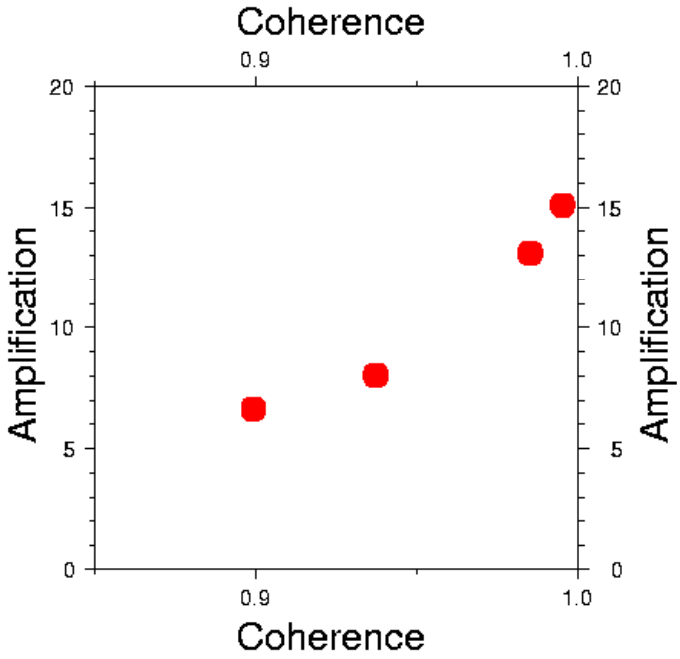

Figure 6. Comparison of the relationship between coherence and amplification for the dominate component of the pure SV and SH incident waves and the random incidence waves for the 3D model. The values shown are from Table 3 at 1.7 Hz, which is the resonant frequency of the basin.

4 DISCUSSION

It was observed from the recorded earthquakes that there is a positive correlation between the coherence and amplification of the waves in the basin. Our original intention was to evaluate the coherence of the incident waves, not the waves inside the basin, which would be affected by scattering within the basin. Initially coherence functions were calculated using the recordings from the rock sites P22 and P25, but it was found that the coherence between the recordings at these two sites was not significantly better than background noise. This probably was due to the large separation between the two sites (350 m). Wavefields in this area may not be coherent for a separation of this distance. As an alternative, the coherence in this study has been calculated using recordings from the 3 pairs of soil sites in the basin. The distance between the two sites in each pair of sites is about 25 metres. The coherence calculated using the recordings from the soil sites inside the basin includes two parts, that of the incident waves and also the scattered waves inside the basin. From the observations it is not certain that the coherence in the basin reflects the coherence of the incident waves. However the 3D modelling of pure and random wavefields showed that coherent incident waves were amplified more in the basin than waves of less coherence.

This difference in amplification for the waves of different coherence may be due to the destructive interference of the random waves propagating inside the basin. The resonant amplification in the soil layer is due to the superposition of the waves bouncing back and forth between the ground surface and the basement, and when the waves are in phase, the superposition will produce a greater amplification. The complex random waves have less chance to be in phase and to produce the same amplification as the coherent waves do. Therefore we see that the coherent waves are amplified more in a basin than random waves.

The degree of incoherence, or randomness, of the incident waves may be related to the scattering along the path. The scattering may produce complex secondary waves as well as reducing the dominant contribution of the original waves in the total wavefield. This would result in the decrease of coherence in the total incident wavefield. The more scattering the incident waves experience, the less they are coherent, and hence the less they would be amplified in a basin. If the degree of scattering is dependent on path length, the incident waves

from a very local earthquake would tend to be amplified more than from a distant earthquake, as they would experience less scattering along the short path. Haines & Yu (1997) showed in the case of the Alfredton basin that the wavefields from distance earthquakes were less coherent than from nearby earthquakes. Thus using distant events to estimate the amplification of a site may underestimate the amplification for some local events.

5 CONCLUSIONS

A correlation between the amplification and spatial coherence in the observed seismic data from the Parkway basin has been found and the correlation is supported by three dimensional computer modelling. The modelling reveals that highly coherent waves tend to be amplified more in a resonant basin than random waves. The implications of this result are that waves from a local earthquake may tend to be amplified more than a distant earthquake, as the waves from a local earthquake would experience less scattering on their short path to the observation site and hence they would be more coherent.

6 ACKNOWLEDGEMENTS

This study has been funded by the EQC Research Foundation. Thanks are due to FRST for funding the data collection and initial analysis. The authors also thank John Haines of Cambridge University for his advice on the three-dimensional modelling.

REFERENCES:

Barker, P. R. 1996. A report on cone penetrometer and seismic cone penetrometer testing at Parkway -- Wainuiomata. Barker Consulting, P. O. Box 27-106, Wellington, New Zealand.

Beetham, R. D. 1999. Microzoning project Parkway Basin subsurface investigations, Wainuiomata. Institute of Geological & Nuclear Sciences science report 99/14.

Begg, J. G., Mildenhall, D. C., Lyon, G. L., Stephenson, W. R., Funnell, R. H., Van Dissen, R. J., Bannister, S., Brown, L. J., Pillans, B., Harper, M. A., and Whitton, J. 1993. A paleoenvironmental study of subsurface Quaternary sediments at Wainuiomata, Wellington, New Zealand, and tectonic implications. *N Z J. Geol Geophys*, Vol 36 461-473.

Chavez-Garcia, F. J., W.R. Stephenson and M. Rodriguez 1999. Lateral propagation effects observed at Parkway, New Zealand. A case history to compare 1D versus 2D site effects, *Bull. Seism. Soc. Am*., Vol 89 718-732.

Duggan, E. B. 1997. Shallow seismic structure of Parkway Basin, Wainuiomata, New Zealand. B. Sc. (Hons) thesis, School of Earth Sciences, Victoria University of Wellington, New Zealand, 116p.

Field, E. H., and K. H. Jacob 1995. A comparison and test of various site-response estimation techniques, including three that are not reference-site dependent, *Bull. Seism. Soc. Am.,* Vol 85 1127-1143.

Haines, A. J. and J. Yu 1997. Observation and synthesis of spatially-incoherent weak-motion wavefields at Alfredton Basin, New Zealand, *Bull. NZ Natl. Soc. Earthquake Engineering*, Vol. 30(1) 14-31.

Sutherland, A. J., and Logan T. C. 1998. SASW Measurement for the Calculation of site amplification. EQC research project 97/276. Central Laboratories Report 98-522422, Opus Institutional Consultants, Lower Hutt, New Zealand.

Yu, J. 1996a. Observation and synthesis of seismic wavefields in basin structures, PhD thesis, Victoria University of Wellington.

Yu, J. 1996b. Processing of data from a seismic experiment in Parkway, Wainuiomata. Institute of Geological & Nuclear Sciences science report 96/10, 372p.

7 RETURN TO INDEX